INDIAN JOURNAL OF SCIENCE AND TECHNOLOGY

RESEARCH ARTICLE

Bio-Sorbent of Silica Ash from Palm Frond for Elimination Chromium (VI) from W ater Sources

Fatima A Al-Qadri[1]*, Raiedhah Alsaiari[2], Mervate Mohamed Mohamed[3], Esraa Mohamed[3], Faeza Alkorbi[3], Norah Alsaiari[3], Moustafa A Rizk[2]

1 Professor of Empty Quarter research Unit, Department of Chemistry, College of science and art in Sharurah, Najran University, Kingdom of Saudi Arabia
2 Associate Professor of Empty Quarter research Unit, Department of Chemistry, College of science and art in Sharurah, Najran University, Kingdom of Saudi Arabia
3 Assistant professor of Empty Quarter research Unit, Department of Chemistry, College of science and art in Sharurah, Najran University, Kingdom of Saudi Arabia

OPEN ACCESS

Received: 31-12-2023
Accepted: 04-02-2024
Published: 29-02-2024

Citation: Al-Qadri FA, Alsaiari R, Mohamed MM, Mohamed E, Alkorbi F, Alsaiari N, Rizk MA (2024) Bio-Sorbent of Silica Ash from Palm Frond for Elimination Chromium (VI) from W ater Sources. Indian Journal of Science and Technology 17(11): 979-989. https://doi.org/10.17485/IJST/v17i11.3275

* **Corresponding author**.

fatimaalqadri@gmail.com

Funding: Deanship of Scientific Research at Najran University for funding this work, under the Research Groups Funding program grant code ((NRP/SERC/12/1).

Competing Interests: None

Published By Indian Society for Education and Environment (iSee)

ISSN
Print: 0974-6846
Electronic: 0974-5645

Abstract

Objectives: This study describes the creation of a low-cost silica material using a silicate extract as a precursor. The main objective of this work is to develop an inexpensive sample to use as green removal for toxic heavy metals from water sources. **Methods:** This work produces Silica ash from combustion palm frond as waste ash through a simple calcination process at 500°C and a green extraction with water. Nitrogen adsorption-desorption of the ash has done, FTIR analyses, and transmission electron microscopy were used to characterize the samples. Adsorption Cr(VI) equilibrium data onto silica ash was done by Batch process using 0.25 g of waste palm frond ash silica and 100 mL of solutions with varying beginning Cr(VI) concentrations ranging from 100 to 400 mg/L at 70 °C, normal pH, and continuous stirring for 24 hours at a constant agitation speed. The effect of different conditions pH, temperatures, initial concentrations, dosage, and time on the adsorption capacity were investigated. The adsorption isotherms were fitted using Langmuir and Freundlich models, the adsorption kinetics were evaluated using pseudo-first order and pseudo-second order models also thermodynamic parameters were calculated. **Findings:** The extracted silica FTIR spectra were analyzed with main characteristic peaks at 500–1590 and 490–510 cm were assigned to (Si-O-Si), (Si-OH). N_2 adsorption isotherm of the functionalized silica gave a hysteresis loop in the range of p/p° between (0.5 and 1). The resulting mesoporous silica ash material had a surface area of 226.36 m^2/g and pore sizes of 6.7 nm. This low-cost silica ash-based adsorbent has a maximum Chromium Cr(VI) adsorption capacity of (83.79 mg/g) values. The removal of Cr(VI) was between 97% and 98 % by was for all used factors, the Adsorption obtained capacity q_{max} (mg/g) by Langmuir was 58.87 mg/g and the n value obtained by Freundlich isotherm was 1.1. The negative results of thermodynamic parameters for adsorption of Chromium (VI) onto silica surface values suggested that the adsorption process was spontaneous and that the adsorbate's state at the solid/solution interface

became less random and the values obtained were ΔS (**-151.6** J.mol^{-1}), ΔH° (-18.88 J.mol^{-1}), and ΔG°(**- 1797** J.mol^{-1}). **Novelty:** The results show that produced silica from palm waste ash has a strong capability for eliminating toxic metals as Chromium (VI) as a low-cost alternative to commercial adsorbent.

Keywords: Palm frond; Silica; Chromium (VI); Adsorption; Kinetic; Thermodynamic; Waste ash

1 Introduction

Among the most vital natural resources on Earth, water makes the most valuable resource. It is essential to all civilizations' ability to grow sustainably[1]. Heavy metals, such as As, Pb, Cr, Hg and Ni, are non-biodegradable, toxic and persist in the environment due to their bioaccumulation tendency causing severe health issues to live organisms upon entering the food chain[2]. The chemical industry produces a wide range of chemical compounds because of the quick progress in research and technology[3]. Both the rate of release and the concentration of these dangerous substances in the environment are rising. Among the most common contaminants found in water, Cr, primarily as Cr(VI), is produced by the mining, metal finishing, textile, electroplating, and leather industries[4,5]. The acceptable and allowable Cr(VI) concentrations in drinking water and industrial wastewater are 0.05 mg/L and 0.5 mg/L, respectively, according to WHO regulations[5]. Cr(VI) can enter the human body through the skin and oral routes and is extremely soluble in water. It must be eliminated from the effluents before disposal because it is very hazardous and carcinogenic when exposed over an extended period[6]. The palm tree belongs to the family Arecaceae of evergreen plants. About 40 kilograms of burnable waste are produced annually by each date palm tree. Date-producing nations' environments are contaminated by the burning of date palm trash on fields or its disposal in landfills. Numerous thermal, biochemical, and physiochemical processes are available for the long-term use of date palm biomass. Date palm has a low moisture content and a high volatile solid content as well. Date palm leftovers are a great biomass resource in nations that produce date palm because of these reasons[7]. According to numerous studies, Saudi Arabia alone produces more than 200,000 tons of date palm biomass each year. Date palm wastes include date pits, dried frond bases (karab), fronds, and offshoots. Local farmers say that this waste is usually gathered and burned. A small portion of the trash is diced up and combined with other biowaste to be used as animal feed, or it is left to naturally decompose and be used as fertilizer[8]. With an emphasis on the fronds in particular, numerous studies have looked at the capacity of date palm debris to absorb heavy metals. Mature fronds have a rachis, leaflets, and thorns, and they are arranged in two spirals around the trunk, one left-handed and one right-handed[9]. The purpose of this study is to show applied and novelty of silica ash made from palm fronds can be used for the removal and purification of heavy metal-polluted water sources, as well as for the best treatment of environmental pollution issues through the use of eco-friendly and safer methods that will benefit both human life and the economy. SEM, BET, and FTIR analysis were used. The effects of solution pH, ligand mass, metal ion concentration, and shaking time on the preconcentration process were studied. The adsorption behavior and functional properties of these low-cost bio-sorbents were investigated through the adjustment of process parameters. Kinetics and thermodynamic studies have been used to investigate the underlying mechanism.

2 Materials and Methodology

2.1 Materials

Chemical reagents like oxalic acid and ($K_2Cr_2O_7$) from a chemical reagent company were purchased from a chemical reagent company. All the reagents were of analytical grade. Palm frond waste ash (PFWA) was made on-site by gathering palm tree leaves in Sharoura City, Najran, Kingdom of Saudi Arabia, and using them as a raw material to make silica ash by burning them in an oven. A sustainable, accessible, and secure source of silica is PFWA. PFWA is now disposed of in landfills, which is a problem for the environment because it contaminates the ecosystem today and in the future. The fact that PFWA contains 46.0 percent silicon makes it possible to extract silica from palm ash. A chemical reagent supplier sold other chemical reagents such as $K_2Cr_2O_7$ and oxalic acid. Distilled water of the analytical grade served as each reagent.

2.2 Preparation of Silica Adsorbent

In this investigation, silica from palm was extracted and functionalized using oxalic acid as a leaching agent. The leaves and fronds of local palm trees were gathered in Sharoura City, Najran, Saudi Arabia. After being thoroughly cleansed with distilled water, the leaves were dried for several hours before being sliced into little pieces. The material was ground using an electric blender into a soft powder, sieved, and kept in a plastic container until it was utilized in the studies. An exact amount of oxalic acid solution can be found in a 500-ml beaker after adding 10 g of palm frond powder (with an average particle size of 75 m) to it. The solution's temperature was measured while the beaker was on the hot plate with the magnetic stirrer, then the solution's temperature was increased to 70°C. The reaction time was 90 minutes on record. After the acid leaching procedure, the oxalic acid content of the palm ash was eliminated by rinsing it with distilled water at room temperature. Before being burned for 30 minutes at 800 °C in the furnace, the materials were dried for two hours at 60 °C in the oven.

2.3 Chromium (VI ions)

Stock solutions of chromium (VI) as metal ions had been prepared by dissolving ($K_2Cr_2O_7$) in distilled water. The stock solution containing 1000 $mg.L^{-1}$ of Cr(VI) was prepared by dissolving 3.73 g of A. R. grade K_2CrO_4, $2H_2O$ in 1000 ml double distilled water. Required initial concentration of Cr(VI) standards were prepared by appropriate dilution of the above stock Cr(VI) solution.

2.4 Instrumentation and characterization

For spectrophotometric measurements, a Perkin-Elmer Lambda 35 spectrophotometer with 1.0 cm^3 quartz cells (scan speed, 8 nm/sec) was used. The pH was measured using a Jenway 3305 pH meter with a glass-calomel electrode assembly that was accurate to 0.01 pH units. The pH-meter was calibrated using buffers with pH values of 4.0 and 10.0 (prepared by dissolving buffer capsules in a definite amount of second-generation de-ionized water). A Jenway 1000 magnetic stirrer was used to stir the solutions. The surface functional groups of the samples must be determined. For spectrophotometric measurements, a Perkin-Elmer Lambda 35 spectrophotometers with 1.0cm quartz cells (scan speed, 8nm/sec) was used. Jenway 3305 pH-meter accurate to 0.01 pH unit with glass calomel electrode assembly was used to measure the pH. The pH-meter was calibrated using buffers with pH values of 4.0 and 10.0 (prepared by dissolving buffer capsules in definite amount of second de-ionized water). Jenway 1000 magnetic stirrer was used to stir the solutions. It is necessary to identify the samples' surface functional groups. Analyzer for surface area and pore size (Quantachrome Instruments). Nitrogen (N_2) adsorption-desorption isotherms at 77.5 K were measured using a NOVA 2200e surface area and pore size analyzer (Quantachrome Instruments). The sample's specific surface area was calculated using the BET (Brunauer-Emmett-Teller) method, and the pore size distribution was examined.

2.5 Adsorption by Batch Experiments

Using 100 mL of Cr(VI) solutions and 0.25 g of palm frond silica ash, batch studies were carried out with initial Cr(VI) concentrations ranging from 100 to 400 mg/L. These were put in different conical flasks, and constant stirring was done for 24 hours at 70°C and a normal pH to allow for adsorption to occur. Using the following formula, the equilibrium adsorption capabilities of palm silica ash for Cr(VI) were determined: solution for cleaning polluted areas of metal. To prevent any discrepancy in the experimental results, all investigations were conducted in triplicate, with relative deviations and reproducibility of roughly 2.5% and ±0.5%, respectively. Using the following formula, the equilibrium adsorption capabilities

of palm silica ash for Cr(VI) were determined:

$$q_e = \frac{(C_i - C_e)}{W} \times V \quad (1)$$

where q_e is the equilibrium adsorption capacity (mg/g); C_i and C_0 are the initial and equilibrium concentrations (mg/L) of the Cr(VI) solution, respectively; v is the volume of the initial solution (L) used for sorption; and W is the weight of the adsorbent (g). The effects of various parameters on the rate of adsorption process were observed by varying contact time, initial concentration of chromium ion, adsorbent doses, and initial pH of solution. After adsorption, the residual concentration of chromium was filtered by using Whatman filter paper then the filtrate determined by spectrophotometer. Using the following equation, the percent removal (% R) of Cr(VI) ions was determined [2]:

$$Removal\ (\%\ R) = \frac{C_o - C_i}{C_o}\ x\ 100 \quad (2)$$

2.6 Kinetic Adsorption

The kinetic reaction occurred, and the equilibrium time was determined utilizing 0.5 g of sorbent at 70 °C. The adsorption time varied from 30 to 120 min. The kinetics adsorption was estimated by two kinetic models: the pseudo-first order model and pseudo-second order model.

3 Results and Discussion

3.1 FTIR Analysis for Cr(VI) Adsorption

The effects of Cr(VI) adsorption on the vibration frequency of the functional groups of the adsorbents were studied using Fourier transform infrared spectra (FTIR). KBr of spectroscopic grade was separately combined with each fresh and Cr(VI)-loaded adsorbent before being formed into pellets at a pressure of approximately 1 MPa. The pellets had a thickness of 1 mm and a diameter of roughly 10 mm. Next, the adsorbents were examined in the 1000–400 cm^{-1} spectral range. The FTIR spectra are shown in Figure 1. Other adsorbents also produced spectra of the same sort. These spectra revealed a multitude of absorption peaks, demonstrating the adsorbent's complexity. One of the crucial elements to comprehend the mechanism of metal binding on natural adsorbents is the functional group. The two primary distinguishing peaks, 500–1590 and 460–524 cm were attributed to respectively, (Si-OH), (Si-O-Si), and (Si-O-Si) [10]. And in the FT-IR plots, the change in the prominent peak's wave number related to the fresh and Cr(VI)-loaded adsorbents is depicted. These changes in wave length indicated that there was a metal binding process occurring at the adsorbents' surface. Numerous absorption peaks may be seen in the spectra, which highlights how complex natural adsorbents are. Wave number changed significantly from 1500.78 cm-1 to 3055.24 cm^{-1} (metal loaded palm frond loaded). This result comparing with other similar previous work reported a FTIR spectrum of peanut shells presenting similar bands (Zhao et al. [11]).

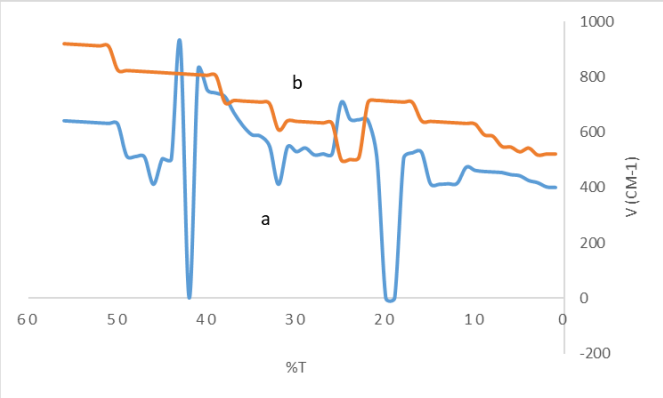

Fig 1. FTIR of: (a) Activated silica ash free, (b) Cr(VI)

3.2 Scanning Electron Microscope (SEM)

Petroleum wax was used to fix waste palm frond samples to a glass plate, and then a small layer of gold was sprayed on top for SEM analysis. On the surface of the palm frond, gold particles were deposited in the vacuum chamber of the gold depositing machine. The glass plate was also made conductive using particular conductive solutions. Scanning electron micrographs of palm frond surfaces before they were burned and reduced to ash are shown in Figure 2. The findings showed that the palm frond's surface was uneven and rough (Figure 2**a**). The shape of palm frond ash was dramatically altered after calcination, and asperities on its surface were almost eliminated (Figure 2 **b**). The morphology of silica prepared from pretreated palm fronds.

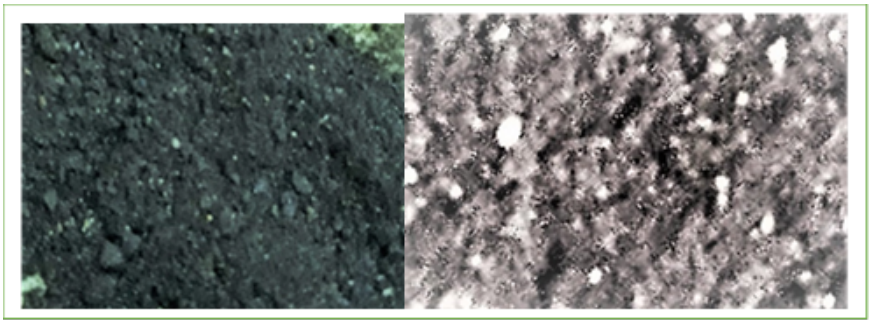

Fig 2. SEM images of (a), palmfrond SiO_2 (b) silica ash after adsorption of Cr(VI)

3.3 Nitrogen Adsorption Desorption Analysis

3.4 Effect of contact time on adsorption efficiency

The relationships between Cr(VI) adsorption efficiency and time, as well as between Cr(VI) adsorption capacity and time, are depicted in Figure 3. The adsorption efficiency and capacity of Cr(VI) increased with time, as Figure 3 illustrates. There were two phases to the adsorption of Cr(VI) by palm silica ash: the first reaction stage, which lasted from the start to the end of the thirty minutes; the silica ash surface absorbed 99 percent of the Cr(VI) ions after 30 minutes of contact; this result also shows the percentage of Cr(VI) ions removed, as well as the second phase. Surface adsorption was the main reaction in the first stage, which accelerated the adsorption reaction and enhanced its capacity and efficiency. The adsorption reaction was comparatively slow in the second reaction stage and was dominated by gradual adsorption. After 90 to one 150 minutes, it steadily came to rest. Cr(VI) is readily adsorbed by palm silica ash, a mesoporous material, due to its abundance of active sites and high mass transfer driving force during the early stages of adsorption. Nonlinear adsorption results from the accumulation of a significant amount of Cr(VI) on the surface of palm silica ash over time, which decreases the number of active sites and impedes Cr(VI) movement. These findings are consistent with previous research; Rajni Garg[(2)] noted a similar pattern in the adsorption of Cr(VI).

3.5 Effect of Adsorbent Dosage

As the adsorbent dosage was increased from 1 to 4 g/100 mL, the removal percentage of Cr(VI) increased quickly, reaching 98% at the 4 g/100 mL dosage. There was no additional increase in Cr(VI) adsorption with increasing adsorbent dosage after the removal efficiency progressively achieved adsorption equilibrium at a dosage of 2 g/100 mL. The adsorption potential of an adsorbent at a particular starting concentration is largely dependent on the adsorbent dosage. Because certain adsorbent active sites remained unsaturated during the adsorption process, the adsorption capacity fell from 4 mg/g at 1 g to 1.22 mg/g. Between 97 and 98 percent of the Cr(VI) ions were eliminated during the adsorption process. The accessible adsorption sites may be the main cause of the difference in adsorption capabilities at various adsorbent dosages. As the adsorbent dosage rose, more surface area and active sites became available for adsorption. Because it added unavailable sites, the increased adsorbent dosage had no effect on adsorbate uptake once adsorption reached equilibrium[(12)]. Moreover, although the equilibrium concentration of Cr(VI) was lower, the increased adsorbent dosage increased the interference of the adsorbent surface among the active groups. This occurred because there was insufficient driving force for the adsorbate to spread and bind to the adsorbent surface. These results are in line with earlier studies; Vu et al.[(4)] observed a comparable pattern in the adsorption of Cr(VI).

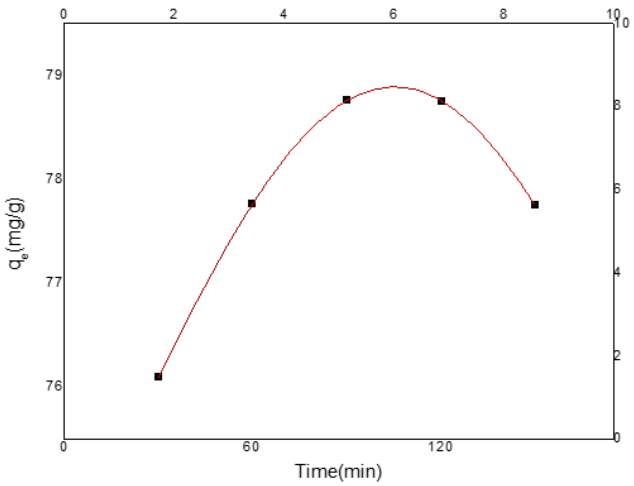

Fig 3. Effect of contact time on Adsorption of Cr(VI) onto silica ash

3.6 Adsorption isotherms

Isotherms illustrate the equilibrium relationship between the concentration of adsorbate in the solution and the amount adsorbed on the adsorbent surface at a constant temperature. To fit experimental adsorption data, a variety of adsorption models are available in the literature. The adsorption isotherm displays the distribution of adsorption molecules between the liquid and solid phases once the adsorption process has reached an equilibrium condition. Finding an appropriate model that may be utilized for design purposes requires fitting the isotherm data to various isotherm models. The equilibrium adsorption isotherm of Cr(VI) ions over palm silica ash is shown in the results. It indicates that the adsorbed amount increases very little with increasing concentrations, showing a vertical increase at low concentrations and a horizontal plateau at higher values. As the initial Cr(VI) concentration rose, the adsorption capacity at equilibrium (q_e) increased from 42.65 mg/g to 83.79 mg/g. Cr(VI) ions reached a high concentration of 16.5 mg/g, at 30 mg/L and then continued to rise to 20 mg/g at 40 mg/L decreased to 12.4 mg/g Cr(VI) ion adsorption rose as the mass transfer driving force increased with initial concentration, in the same way as [13]. Similarly, effect of Adsorption of Chromium (VI) onto Freshwater Snail Shell-Derived Bio- sorbent from Aqueous Solutions as in [8].

3.7 Effect of pH

The influence of solution pH on the adsorption of Cr(VI) ions onto silica ash is demonstrated by the results. The test is carried out in the pH range of 2.0 to 9, since Cr(VI) ion precipitation is anticipated when the pH exceeds 5.0. The adsorption capacity of Cu(II) increased as pH increased, as seen in Figure 5, suggesting that pH has a major effect on Cr(VI) ion adsorption performance. When the pH of the solutions increased from 2 to 9, the elimination of the Cr(VI) ion at equilibrium increased from 98.6 percent to 98.09 percent. When pH is less than 9.0, the Cr(VI) ion adsorption performance on silica ash is low. The elimination of Cr(VI) ions worked best at pH 9. Research demonstrates similar outcomes [14].

3.8 Effect of Temperature

Chromium (IV) ions were adsorbed onto generated silica ash at 70, 80, 90, and 120 °C, with an initial solution concentration of 40 mg./L. The quantity of metal ions (chromium IV) that adsorbed onto silica ash increased with temperature, as demonstrated by the increase from 19.79 mg/g at 70 °C to 22 mg/g at 80 °C. The adsorbent's degradation resulted in a modification of its surface chemistry, which aided in lowering the adsorption of heavy metal ions and increasing the availability of the active functional groups. Additionally, the bonds were twisted, and the desorption process was conducted at higher temperatures [15]. As the temperature rose, the metal ions escaped to the surface, causing the boundary layer to thin Solution phase.

3.9 Adsorption Isotherms

The Langmuir and Freundlich models of isotherms were used to generate the adsorption isotherms. As demonstrated in Figures 4 and 5, these two models were suitable for the process of Chromium (IV) adsorption on the silica made from Palm frond waste ash. Table 1 is a list of the data outcomes. The R^2 values were used as the correlation coefficients in the isotherm equations that described the adsorption process. This study made use of the Freundlich isotherm and Langmuir models.

3.10 Langmuir Isotherm

While the Freundlich isotherm is an experimental equation used to represent heterogeneous systems, the Langmuir isotherm is based on the assumption of homogeneous adsorption. The findings showed that, for the adsorption examined in this work, the Langmuir model performed better than the Freundlich model. This implied that there was homogeneity in the adsorption process. The highest Cr(VI) adsorption capacity measured was 58.87 mg/g, exceeding or matching results from earlier publications (Table 1). Plotting C_e / q_e against Ce produced a straight line with a slope of $1/q_e$, as seen in Figure 4. A correlation coefficient R^2 of 0.97 indicates that the results of the adsorption of Cr(VI) ions onto silica generated by palm silica ash were well fitted using the Langmuir isotherm. The Langmuir constants, b and q_{max}, which were associated with the adsorption energy and maximum adsorption capacity, respectively were computed using the slope and intercept. The following formula represents the Langmuir isotherm, which shows monolayer adsorption described by the following equation [3]:

$$\frac{c_e}{q_e} = \frac{1}{q_{max}.b} + \frac{1}{q_{max}} . C_e \tag{3}$$

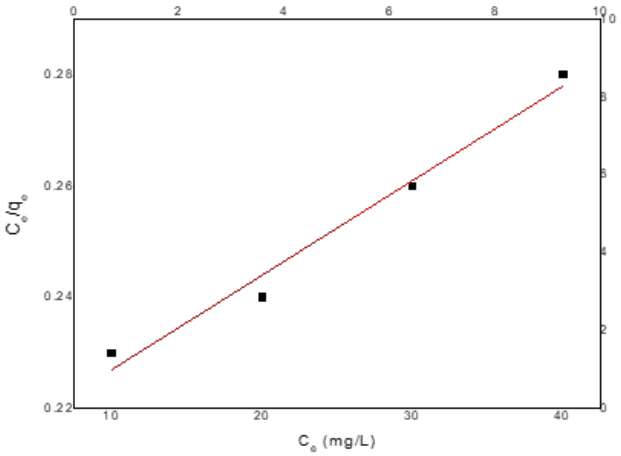

Fig 4. Langmuir isotherm adsorption of Chromium (IV) onto silica surface

The essential characteristics of the Langmuir isotherm can be expressed in terms of a dimensionless equilibrium parameter (R_L). This parameter is defined as follows;

$$R_{L=} \frac{1}{bCi} \tag{4}$$

where C_i is the initial concentration of Chromium (IV). The R_L value indicates that the adsorption is unfavorable: $R_L > 1$; linear: $R_L = 1$; favorable: $0 < R_L < 1$; or irreversible: $R_L = 0$. Table 3 lists the Langmuir and Freundlich isotherm model parameters and correlation coefficients for the adsorption of Chromium (IV) ions on palm silica ash. R_L was found to be 0.0037, 0.00018, 0.00012, and 0.0092. These results emphasized that the Langmuir isotherm was the best at describing the adsorption of Chromium (IV) ions on the prepared silica ash. The values of R_L were in the range of 0–1, which indicated that the adsorption of Chromium (IV) metal cations onto the prepared silica ash was favorable.

3.11 Freundlich Isotherm

The Freundlich isotherm, where C_e denotes the equilibrium concentration mg and qe denotes the amount adsorbed per amount of adsorbent at equilibrium mg/g, is referred to as an experimental model. The Freundlich constants, $K_{f,}$ and n stand for

the adsorption intensity and capacity, respectively. They rely on the adsorbate as well. Plotting ln q_e versus log C_e yields the Freundlich equilibrium constants K_f and n, which result in a straight line with a slope of n. If n is in the range of 1 and 10 (1/n is less than Adsorption is linear if n = 1 and occurs during a chemical reaction if n = 1. While n values between 1 and 10 indicate perfect adsorption, the most common state is one where n > 1, which explains how active centers are dispersed on the surface and any factor that decreases adsorbent-adsorbate interaction as surface density increases. It suggests that the adsorbent has a heterogeneous surface and an easy adsorption mechanism. Therefore, multilayer sorption can be applied to the isotherm. Furthermore, the nonlinearity between them is indicated by the n value. The present study's n value, which varied from 1 to 10, revealed the physical adsorption of metal ions onto the silica fume ash. The values of the Freundlich constants are shown in Table 1; n is 1.11 and K_f is 1.91. K_f and n, the Freundlich constants, were found using Equation (4) these results are similar to research reported in [16].

$$logq_e = logK_f + \frac{1}{n} logc_e \tag{5}$$

Table 1. Parameters of Langmuir and Freundlich isotherms for adsorption of Chromium (IV) ions onto silica surface

Isotherm model	Evaluated parameters of isotherm		
Langmuir	q_{max} **(mg. g $^{-1}$)**	b **(L.mg $^{-1}$)**	R^2
	58.87	0.08	0.97
Freundlich	n	K_f	R^2
	1.11	1.91	0.98

3.12 Adsorption Kinetics

Pseudo-first order kinetic models can be used by the following equation.

$$ln(q_e - q_t) = lnq_e - k_1 t \tag{6}$$

where q_e and q_t (mg/g) are the amounts of Chromium (IV) ions adsorbed onto silica extracted from palm waste ash at equilibrium and time t, respectively; and K_1 (min^{-1}) is the rate constant of the pseudo-first order kinetic model. A straight line was obtained by plotting ln (q_e-q_t) against t.

A straight line was obtained by plotting ln (q_e-q_t) against t. This straight line was used to determine k_1, correlation coefficient R^2, and the theoretical value of q_e. Rate constant value k_1 was obtained from the linear plots of ln ($q_e - q_t$) versus t from slopes shown in Figure 5. The correlation coefficient values obtained were relatively small and the experimental q_e values did not match the computed values that were derived from the linear plots, as Table 2 illustrates. This demonstrates that the pseudo-first order equation was not followed in the adsorption of Cr(IV) onto the silica ash. Despite the linear plot and non-linearity between the calculated (q_e,calc.) and experimental (q_e,exp.) values, the pseudo-first order kinetic model's correlation coefficient values were smaller than those of the pseudo-second order kinetic model. As a result, the pseudo-first order kinetic model's adsorption kinetics were subpar. [17]

1. **Pseudo-second order reaction**

In chemical reactions where electrons are shared or exchanged between the adsorbent and adsorbate due to valence forces, the pseudo-second order kinetic model of the adsorption mechanism is required [18]. Using the relationship below, the equilibrium adsorption was assessed. The pseudo-second order model equation is given as follows:

$$\frac{t}{q_t} = \frac{1}{k_2 q 2_e} + \frac{1}{q_e} . t \tag{7}$$

Pseudo-second order kinetic model's rate constant (g.mg^{-1}min^{-1}) k_2. The values of k_2 and q_e, calc were calculated using the straight-line plots of t/qt against t Figure 5. The behavior across the entire contact time range was more likely to be predicted by this model. The R^2 value for the pseudo-second order kinetic model was very close to or even equal to one, as shown in Table 2. The calculated equilibrium adsorption capacity values (q_e, calc.) were extremely close to the experimental (q_e, exp.) values, providing further evidence that the Chromium (IV) ion adsorption process onto prepared silica ash matched the pseudo-second-order model kinetics.

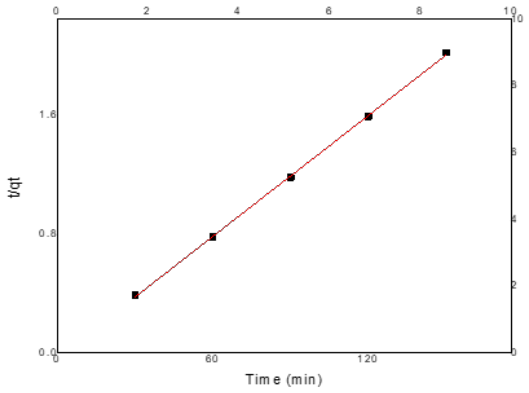

Fig 5. Adsorption of Chromium (IV) ions onto silica surface Pseudo-second order

Table 2. Kinetic parameters and correlation coefficients of two kinetic equations for different initial Chromium (IV) ion concentrations on silica surface

Metal ion	$q_{e,exp}$ (mg/g)	First-order kinetic mode			Second-order kinetic mode		
		$q_{e,cal}$ (mg.g^{-1})	k_1 (min)	R^2	$q_{e,cal}$ (mg.g^{-1})	k_2(g.g^{-1}.min^{-1})	R^2
Chromium (IV)	7.59	3.266	0.004	0.86	7.14	0.02	0.99

3.13 Thermodynamic Parameters

The standard enthalpy (ΔH°), standard entropy (ΔS°), and standard free energy (ΔG°) changes resulting from the transfer of a unit mole of solute from the solution onto the solid-liquid interface served as the process' thermodynamic parameters. The following equations were used to determine the values of ΔH° and ΔS°:

$$lnkc = \frac{\triangle S}{R} - \frac{\triangle H}{RT} \tag{8}$$

$$\triangle G = -RTlnK \tag{9}$$

where T (K) denotes the absolute temperature in Kelvin, R denotes the universal gas constant (8.314 J. mol^{-1}.K^{-1}, and K_c denotes the linear adsorption distribution coefficient, which is defined as follows: is equal to C_o/C_e, where C_o and C_e mg.L^{-1} are the initial and equilibrium concentrations of the adsorbate still present in the liquid phase, respectively. ΔG is the adsorption free energy, H is the enthalpy change kJ.mol^{-1}, and ΔS is the entropy change J. mol^{-1}.K^{-1}. Table 3 lists the data that were gathered for the thermodynamic parameters. The exothermic character of the adsorption is indicated by the negative value of ΔH°. Furthermore, a negative value of ΔS° suggests that either an associative or dissociative mechanism may be at work during the adsorption reaction. An adsorption process using an associative mechanism is indicated by a negative value for ΔS°. In this instance, the adsorption occurred as a result of the adsorbent and adsorbate forming an activated complex. The entropy ΔS° value's sign indicated that there was a decrease in the degrees of freedom for the Cr(VI) (II) ions in the solution as well as a change in the adsorbate's state at the solid/solution interface throughout the adsorption process, with ΔS° < 0 or > 0. When ΔG° was negative, it meant that the adsorption process was spontaneous. Conversely, when ΔG° increased in value as temperature increased, it meant that the adsorption was not spontaneous and that its saponaceousness was inversely related to temperature. Numerous studies have documented the spontaneous adsorption of Cr(VI) onto bio-sorbents, including peanut shells lignocellulosic nanocomposites and apricot shells.[19]

Table 3. Thermodynamic parameters for adsorption of Chromium (IV) onto silica surface

ΔS° (J.mol^{-1}.k^{-1})	ΔH° (J.mol^{-1})	ΔG° (J.mol^{-1})	T (K)
-151.6	-18.88	-428	343
		-1027	353
		-1056	363
		- 1797	393

Table 4. Comparison of Cr(VI) adsorption capacities with other Biosorbent

Adsorbent	Adsorption capacity (mg/g)	References
Silica Ash from Palm Frond	83.79	The present study
Snail Shell	8.85	VADDI, Dhilleswara Rao, et al., Catalysts. 2022, 12.3: 290 [16]
walnut-derived	75.26	GARG, Rajni, et al Scientific Reports, 2023, 13.1: 6859 [2]
Oil Palm Bagasse and Yam Peels	111.45	VILLABONA-ORTÍZ, et al., Water, 2022, 14.8: 1240 [20]
peanut shells (PSh)	3.49	RZIG, Boutheina, et al Water Science and Technology, 2021, 84.3: 552-575 [21]

4 Conclusion

High-purity silica ash was prepared from palm frond waste ash using oxalic acid as an organic leaching agent instead of inorganic acid. The chemical and structural properties of the silica ash were characterized through various methods, revealing a specific surface area, and pore size of 226.36 m^2/g and pore sizes of 6.7 nm respectively. The adsorption performance of silica ash for removing Cr(VI) from aqueous solutions was then investigated the strength of this research is the Silica ash demonstrated excellent cycle adsorption performance with a dosage of 0.25 g/L, an initial Cr(VI) concentration 40 mg/L, an optimum of 9.0, an equilibrium adsorption time of 150 min, and a chemisorption mechanism following pseudo-second-order kinetics. Cr(VI) adsorption capacity increased with temperature, with an ideal reaction temperature of 120°C. Adsorption was governed by both the Langmuir and Freundlich models, with the maximum theoretical adsorption capacity based on the Langmuir model being 83.79 mg/g. The recommendations and prospects can be elaborated that the adsorption performance of silica ash mesoporous materials was superior although only Cr(VI) was investigated in this study. Future studies are expected to explore the removal of mixed heavy metals from real wastewater. Overall, this study confirms that silica ash from palm fronds is a reliable and low-cost adsorbent for effectively removing Cr (VI) from wastewater. Its high surface area also makes it promising for various applications, including catalysts and adsorbents.

5 Acknowledgement

The authors are thankful to the Deanship of Scientific Research at Najran University for funding this work, under the Research Groups Funding program grant code ((NRP/SERC/12/1).

References

1) Alrowais R, Bashir MT, Khan AA, Bashir MT, Abbas I, Daiem MMA. Adsorption and Kinetics Modelling for Chromium (Cr6+) Uptake from Contaminated Water by Quaternized Date Palm Waste. *Water*. 2024;16(2):1–23. Available from: https://doi.org/10.3390/w16020294.
2) Garg R, Garg R, Sillanpää M, Alimuddin, Khan MA, Mubarak NM, et al. Rapid adsorptive removal of chromium from wastewater using walnut-derived biosorbents. *Scientific Reports*. 2023;13(1):1–12. Available from: https://doi.org/10.1038/s41598-023-33843-3.
3) Ren B, Jin Y, Zhao L, Cui C, Song X. Enhanced Cr(VI) adsorption using chemically modified dormant Aspergillus niger spores: Process and mechanisms. *Journal of Environmental Chemical Engineering*. 2022;10(1):1–9. Available from: https://doi.org/10.1016/j.jece.2021.106955.
4) Vu XH, Nguyen LH, Van HT, Nguyen DV, Nguyen TH, Nguyen QT, et al. Adsorption of Chromium(VI) onto Freshwater Snail Shell-Derived Biosorbent from Aqueous Solutions: Equilibrium, Kinetics, and Thermodynamics. *Journal of Chemistry*. 2019;2019:1–11. Available from: https://doi.org/10.1155/2019/3038103.
5) Esfandiar N, Suri R, Mckenzie ER. Competitive sorption of Cd, Cr, Cu, Ni, Pb and Zn from stormwater runoff by five low-cost sorbents; Effects of co-contaminants, humic acid, salinity and pH. *Journal of Hazardous Materials*. 2022;423(Part A):1–13. Available from: https://doi.org/10.1016/j.jhazmat.2021.126938.

6) Faiad A, Alsmari M, Ahmed MMZ, Bouazizi ML, Alzahrani B, Alrobei H. Date Palm Tree Waste Recycling: Treatment and Processing for Potential Engineering Applications. *Sustainability*. 2022;14(3):1–21. Available from: https://doi.org/10.3390/su14031134.
7) Zafar AU, Shen J, Ashfaq M, Shahzad M. Social media and sustainable purchasing attitude: Role of trust in social media and environmental effectiveness. *Journal of Retailing and Consumer Services*. 2021;63:102751. Available from: https://doi.org/10.1016/j.jretconser.2021.102751.
8) Al-Qadri FA, Alsaiari R. Silica ash from waste palm fronds used as an eco-friendly, sustainable adsorbent for the Removal of cupper (II). *Archives of Environmental Protection*. 2023;49(2). Available from: https://doi.org/10.24425/aep.2023.145894.
9) Kushairi A, Ong-Abdullah M, Nambiappan B, Hishamuddin E, Bidin MNIZ, Ghazali R, et al. Oil palm economic performance in Malaysia and R&D progress in 2018. *Journal of Oil Palm Research*. 2019;31(2):165–194. Available from: https://doi.org/10.21894/jopr.2019.0026.
10) Banerjee M, Basu RK, and SKD. Cu(II) removal using green adsorbents: kinetic modeling and plant scale-up design. *Environmental Science and Pollution Research* . 2019;26:11542–11557. Available from: https://doi.org/10.1007/s11356-018-1930-5.
11) Zhao B, Ren L, Du Y, Wang J. Eco-friendly separation layers based on waste peanut shell for gravity-driven water-in-oil emulsion separation. *Journal of Cleaner Production*. 2020;255:120184. Available from: https://doi.org/10.1016/j.jclepro.2020.120184.
12) Hamadeen HM, Elkhatib EA, Moharem ML. Optimization and mechanisms of rapid adsorptive removal of chromium (VI) from wastewater using industrial waste derived nanoparticles. *Scientific Reports*. 2022;12(1):1–12. Available from: https://doi.org/10.1038/s41598-022-18494-0.
13) Elsayed AE, Osman DI, Attia SK, Ahmed HM, Shoukry EM, Mostafa YM, et al. A study on the removal characteristics of organic and inorganic pollutants from wastewater by low cost biosorbent. *Egyptian Journal of Chemistry*. 2020;63(4):1429–1442. Available from: https://doi.org/10.21608/ejchem.2019.15710.1950.
14) Basnet P, Gyawali D, Ghimire KN, Paudyal H. An assessment of the lignocellulose-based biosorbents in removing Cr(VI) from contaminated water: A critical review. *Results in Chemistry*. 2022;4:1–16. Available from: https://doi.org/10.1016/j.rechem.2022.100406.
15) Mahmudi M, Arsad S, Amalia M, Rohmaningsih H, Prasetiya F. An Alternative Activated Carbon from Agricultural Waste on Chromium Removal. *Journal of Ecological Engineering*. 2020;21(8):1–9. Available from: https://doi.org/10.12911/22998993/127431.
16) Vaddi DR, Gurugubelli TR, Koutavarapu R, Lee DY, Shim J. Bio-Stimulated Adsorption of Cr(VI) from Aqueous Solution by Groundnut Shell Activated Carbon@Al Embedded Material. *Catalysts*. 2022;12(3):1–14. Available from: https://doi.org/10.3390/catal12030290.
17) Huynh PT, Nguyen NT, Van HN, Nguyen PT, Nguyen TD, Van-Phuc Dinh. Modeling and optimization of biosorption of lead (II) ions from aqueous solution onto pine leaves (Pinus kesiya) using response surface methodology. *Desalination and Water Treatment*. 2020;173:383–393. Available from: https://www.deswater.com/DWT_articles/vol_173_papers/173_2020_383.pdf.
18) Idowu AA, Temilade FA, Peter A, Vahidhabanu S, Babu BR. Agro waste material as ecofriendly adsorbent for the removal of Zn (II): Isotherm, kinetic, thermodynamic and optimization studies. *Desalination and Water Treatment*. 2019;155:250–258. Available from: https://www.deswater.com/DWT_articles/vol_155_papers/155_2019_250.pdf.
19) Jimenez-Paz J, Lozada-Castro JJ, Lester E, Williams O, Stevens L, Barraza-Burgos J. Solutions to hazardous wastes issues in the leather industry: adsorption of Chromium iii and vi from leather industry wastewaters using activated carbons produced from leather industry solid wastes. *Journal of Environmental Chemical Engineering*. 2023;11(3):1–14. Available from: https://doi.org/10.1016/j.jece.2023.109715.
20) Villabona-Ortíz A, Tejada-Tovar C, Ángel Darío González-Delgado. Elimination of Chromium (VI) and Nickel (II) Ions in a Packed Column Using Oil Palm Bagasse and Yam Peels. *Water*. 2022;14(8):1–17. Available from: https://doi.org/10.3390/w14081240.
21) Rzig B, Guesmi F, Sillanpää M, Hamrouni B. Modelling and optimization of hexavalent chromium removal from aqueous solution by adsorption on low-cost agricultural waste biomass using response surface methodological approach. *Water Science and Technology*. 2021;84(3):552–575. Available from: https://doi.org/10.2166/wst.2021.233.